photonics

Review

Recent Advances and Outlook in Single-Cavity Dual Comb Lasers

Chenghong Zhang [1,†], Fangrui Qu [1,†], Peiwen Ou [1,†], Haoqi Sun [1], Shi He [1] and Bo Fu [1,2,*]

[1] School of Instrumentation and Optoelectronic Engineering, Beihang University, Beijing 100191, China
[2] Key Laboratory of Big Data-Based Precision Medicine Ministry of Industry and Information Technology, School of Engineering Medicine, Beihang University, Beijing 100191, China
* Correspondence: fubo10@buaa.edu.cn
† These authors contributed equally to this work.

Abstract: Dual-comb spectroscopy as an emerging tool for spectral analysis has been investigated in a wide range of applications, including absorption spectroscopy, light detection and ranging, and nonlinear spectral imaging. Two mutually coherent combs facilitate high-precision, high-resolution, and broadband spectroscopy. Recently, dual combs generated from a single cavity have become compelling options for dual-comb spectroscopy, enabling huge simplification to measuring systems. Here, we review the progress of single-cavity dual comb lasers in recent years and summarize the distinctive advantages of single-cavity dual combs. First, the principles of optical frequency comb and dual-comb spectroscopy are introduced in time and frequency domains. Then, the implementation techniques and typical applications of single-cavity dual comb lasers are discussed, including directional multiplexing, wavelength multiplexing, polarization multiplexing, and space multiplexing. Finally, an outlook on the development of single-cavity dual combs is presented.

Keywords: lasers; single-cavity dual combs; dual-comb spectroscopy; mode-locked lasers

Citation: Zhang, C.; Qu, F.; Ou, P.; Sun, H.; He, S.; Fu, B. Recent Advances and Outlook in Single-Cavity Dual Comb Lasers. *Photonics* **2023**, *10*, 221. https://doi.org/10.3390/photonics10020221

Received: 20 January 2023
Revised: 8 February 2023
Accepted: 16 February 2023
Published: 18 February 2023

1. Introduction

Lasers have promoted a multitude of diverse applications owing to their remarkable spatial and temporal coherence properties. The invention of lasers in 1960 was a milestone in the history of optics and opened up a new era for optical research [1]. Subsequently, a variety of lasers were developed according to the different requirements of applications during years of research. Stable narrow-linewidth lasers are required for high-resolution measurement in light detection and ranging [2,3]. High-power lasers find their utility for precise engraving in material processing [4,5]. Ultrafast lasers have spawned a large number of research fields owing to their high peak power and ultrashort pulse width, such as frequency comb metrology [6–9], the dynamic evolution of solitons [10], and nano-materials application in saturable absorption [11–19]. Besides, ultrafast lasers have promoted various practical applications, including material processing [20–22], fluorescence microscopy [23], and in the medical industry [24,25]. Mode-locking is one of the main methods usedto realize ultrafast lasers with picosecond- or femtosecond-level pulse width. A fixed phase relationship between the longitudinal modes is induced in the laser resonator for periodic interference, ultimately producing a train of pulses [26]. The phase-locked longitudinal modes can further achieve optical frequency combs (OFCs).

OFCs are known as evenly spaced combs of spectral lines in the frequency domain and periodic pulse trains in the time domain. The first OFC was generated from a mode-locked femtosecond laser, which was employed in counting cycles from optical atomic clocks with high accuracy [27]. In 2005, one-half of the Nobel Prize for Physics was awarded to John Hall and Theodor Hänsch for their invention of OFCs, which had a spectacular impact on the fields of precision spectroscopy and optical frequency metrology [28,29]. The OFCs possessing extreme fidelity can act as frequency rulers, as they combine the optical frequency with the radio frequency. The great stabilization of OFCs boosts the development of high-resolution measurements, such as optical atomic clock [30,31], precision distance measurement [32–34], light detection and ranging [35], precision optical frequency metrology [28,29], and astronomical observations [36]. However, the detection of optical signals brings out the challenge of digital electronics. The typical techniques transforming the optical signals into detectable signals include virtually imaged phase array spectrometers [37], comb-cavity Vernier spectrometers [38], and Fourier-transform infrared spectrometers [39]. As a kind of Fourier-transform spectrometer, the dual-comb spectroscopy (DCS) uses two coherent frequency combs with a slightly offset repetition rate to perform ultrahigh-resolution, high-sensitivity broadband spectroscopy [40,41]. The remarkable capabilities that enhance the competitiveness of the DCS are applications such as detection and analysis of greenhouse gases [42–45], spectral light detection and ranging [46–49], nonlinear spectroscopy [50,51], medical laboratory science [52], imaging [53,54], and zero-background photothermal/photoacoustic detection [55–57].

There are many different methods to achieve DCS, including strong modulation of a continuous-wave laser [58], two frequency-locked combs produced by two separated mode-locked lasers [59], two sets of stable Kerr combs formed in the ring resonator [60], and two sets of mode-locked pulses with different repetitions produced in the same mode-locked laser [61]. Compared to the former three methods, the DCS generated from a single cavity possesses a simplified structure and high coherence. The high coherence between single-cavity dual combs is naturally ensured since the same environment experienced by dual combs effectively inhibits the common-mode noise. Despite the significant optimization of structure and cost, there are still some challenges for single-cavity dual combs. For instance, the repetition rate difference is limited and inflexible for adjustment, posing challenges for high-speed measurement. In addition, the low output power of single-cavity dual combs is not conducive to most practical applications. The self-starting and tunable single-cavity dual combs were realized by introducing correction algorithms and mechanical structures. Currently, single-cavity dual-comb lasers find applications in the measurement of absorption spectrum [62], ranging [63–65], and optical fiber sensing [66].

In this study, we mainly review the progress in the research of the dual combs generated from a single cavity. First, we briefly introduce the principles of the OFC and DCS. Then, the multiplexing methods used for realizing single-cavity dual combs are elaborated. The typical results and applications based on single-cavity dual combs are discussed. Finally, our conclusions and perspectives of single-cavity dual combs are presented.

2. Principles of Optical Frequency Comb and Dual-Comb Spectroscopy

The invention of the OFC has boosted the development of precision spectroscopy. As an important spectral technology, the DCS was subsequently proposed to overcome the detection challenge of OFCs. In this section, we aim to make a brief theoretical analysis of the OFC and DCS. First, we describe the properties of the OFC in the time and frequency domains, as well as the stabilization methods of the OFC. Then, the properties of the DCS are discussed in the time and frequency domains, respectively.

2.1. Principles of the Optical Frequency Comb

The OFC is a specific kind of laser, which appears as a series of periodic teeth with critically equal intervals in both the time and frequency domains. In the time domain, the OFC appears as periodic pulses with equal intervals T_r, as shown in Figure 1a [67]. Lights with different frequencies travel at different speeds in the dispersive media, which leads to a stable phase difference φ_{ceo}, between the envelope and the carrier of the pulse. In the frequency domain, the OFC is a series of comb teeth shown in Figure 1b [67]. Each comb can be uniquely determined by the repetition rate f_r and the carrier-envelope-offset frequency f_{ceo}. The nth comb ν_n can be described as:

$$\nu_n = n \cdot f_r + f_{ceo} \tag{1}$$

In other words, ν_n is the linear combination of two degrees of freedom, f_r and f_{ceo}. According to the law of Fourier transform, f_r equals to $1/T_r$, and f_{ceo} is described as $(\varphi_{ceo}/2\pi)\cdot(1/T_r)$. In general, the f_r and f_{ceo} are in the ratio frequency range, while ν_n is in the optical frequency range. Therefore, the OFC builds a bridge between ratio frequency and optical frequency domains.

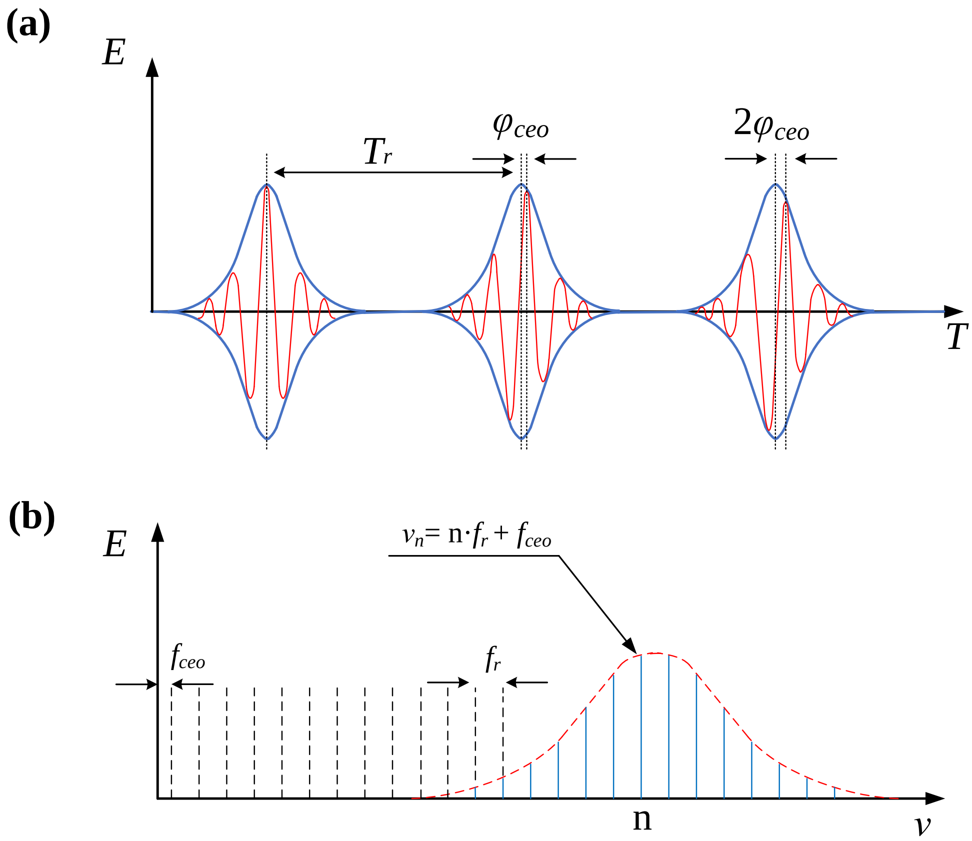

Figure 1. The concept of the OFC. (**a**) Features in the time domain. (**b**) Comb teeth in the frequency domain.

In actuality, the f_r and f_{ceo} of the OFC are unstable due to the interference, making the OFC deviate from the ideal condition. According to the amplification effect, the drift of the f_r and f_{ceo} can be amplified by 10^6 times after mapping to the optical frequency domain. Therefore, it is of great necessity to stabilize the f_r and f_{ceo}. Feedback systems are commonly employed to control the cavity length and the pumping current so that the f_r and f_{ceo} can be stabilized to a standard frequency. The detection of the f_r can be achieved simply through a photodetector, while the f_{ceo} can not be directly detected. The f-$2f$ self-referencing is generally utilized to detect f_{ceo}. Nonlinear media are utilized for frequency doubling, where the f_{ceo} can be acquired from the beat frequency of the n^{th} comb and the $2n^{th}$ comb.

2.2. *Principles of the Dual-Comb Spectroscopy*

The DCS is a kind of technology using two sets of highly coherent OFCs with a small difference in the repetition rate, which can achieve asynchronous optical sampling without mechanical motion scanning. The two OFCs pass through the sample separately, and the spectrum of the OFC can be obtained from the interferogram of dual combs. Each pair of pulses has an increased time delay compared to the previous one due to the difference in the repetition rate of dual combs. The time delay between the interval of every two pairs of pulses can be described as:

$$1/f_r - 1/(f_r + \Delta f_r) = \Delta f_r/(f_r + \Delta f_r) \approx \Delta f_r/{f_r}^2 \tag{2}$$

where f_r is the repetition rate and Δf_r is the difference in the repetition rate. Periodic dislocation and overlap exist between pulses from two OFCs, which generated an interference signal with a period of $1/\Delta f_r$ shown in Figure 2a [42]. The interference of the DCS in the frequency domain is a series of comb teeth with equal intervals in the ratio frequency domain, which are related to the repetition rate difference between two combs. The frequency of the m^{th} comb teeth of the ratio frequency comb can be described as:

$$\nu_m = n \cdot |f_{r1} - f_{r2}| + |f_{ceo1} - f_{ceo2}| \tag{3}$$

where f_{r1} and f_{r1} are the repetition rates of two combs, f_{ceo1} and f_{ceo2} are the carrier-envelope-offset frequency, and ν_m is the beat frequency of two combs in the ratio frequency domain. As shown in Figure 2b [42], the interval between the ratio frequency comb teeth is Δf_r. The DCS maps the spectrum of the OFC to the ratio frequency comb, where the ν_m can be obtained from the fast Fourier transform of interference in the time domain.

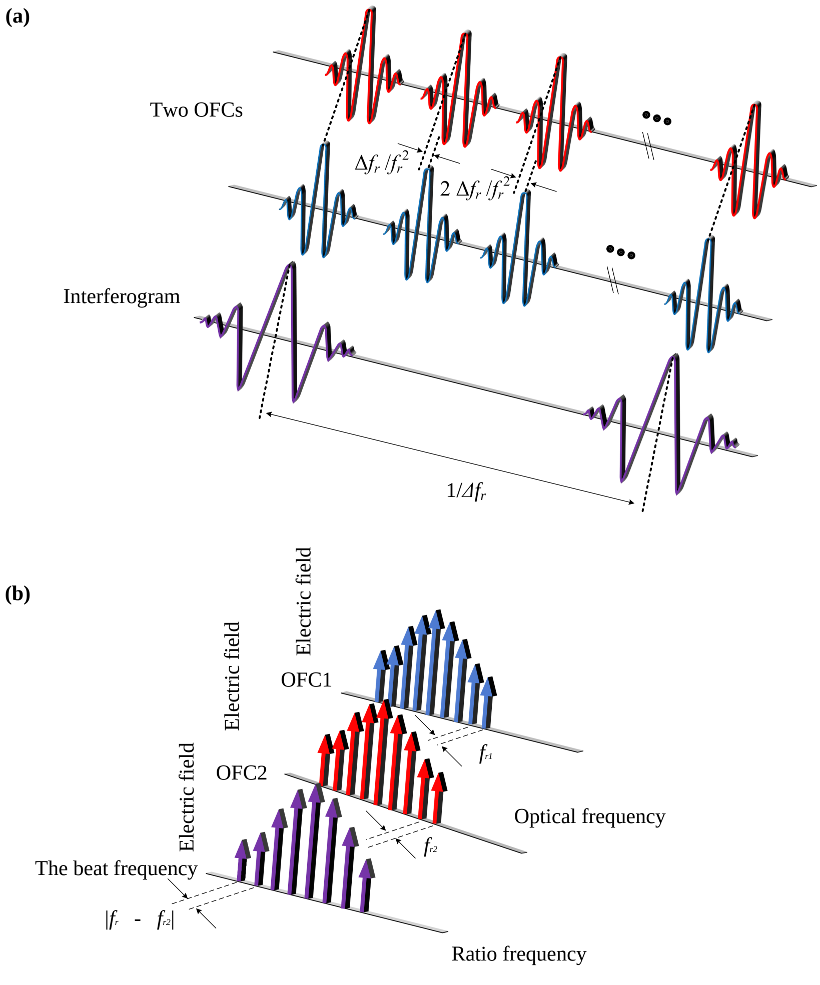

Figure 2. The concept of the DCS. (**a**) The asynchronous optical sampling. (**b**) The beat frequency produced by two OFCs.

3. Single-Cavity Dual-Comb Systems

Dual combs generated from a single mode-locked laser, known as single-cavity dual comb lasers, exhibit remarkable merits of simple structures and low cost. The DCS based on single-cavity dual-comb lasers has been applied in enormous disciplines including gas detection, distance measurement, and fiber sensing. In this section, the four multiplexed methods to generate single-cavity dual combs are summarized, including direction-multiplexing, wavelength-multiplexing, polarization-multiplexing, and space-multiplexing. The principles, advances, and applications of each method are presented in detail, respectively.

3.1. Bidirectional Single-Cavity Dual Combs

Mode-locked pulses can be achieved in the clockwise (CW) and counter-clockwise (CCW) directions in a no-isolator cavity. The difference between the refractive indices of the two directions leads to the repetition rate difference, which results in a free-running dual-comb system.

A typical schematic diagram of the bidirectional dual-comb laser is shown in Figure 3a. In 2008, Kieu et al. firstly reported on an all-fiber bidirectional passively mode-locked laser [68]. Dual-comb lasers based on bidirectional mode-locking have been widely investigated subsequently [69–79]. Generally, the repetition rate difference of bidirectional dual-comb laser is relatively small due to the slight difference of refractive indices between CW and CCW in the same cavity. In 2011, Ouyang et al. proposed a bidirectional dual-comb laser with an obvious repetition rate difference of 6.1 MHz by employing unsymmetrical cavity lengths [80]. In 2018, Olson et al. expanded the bidirectional dual-comb system to the 2-μm band in a Thulium-doped fiber laser. The range of the detuning frequency was broadband tunable from 49.8 to 229.0 Hz [81].

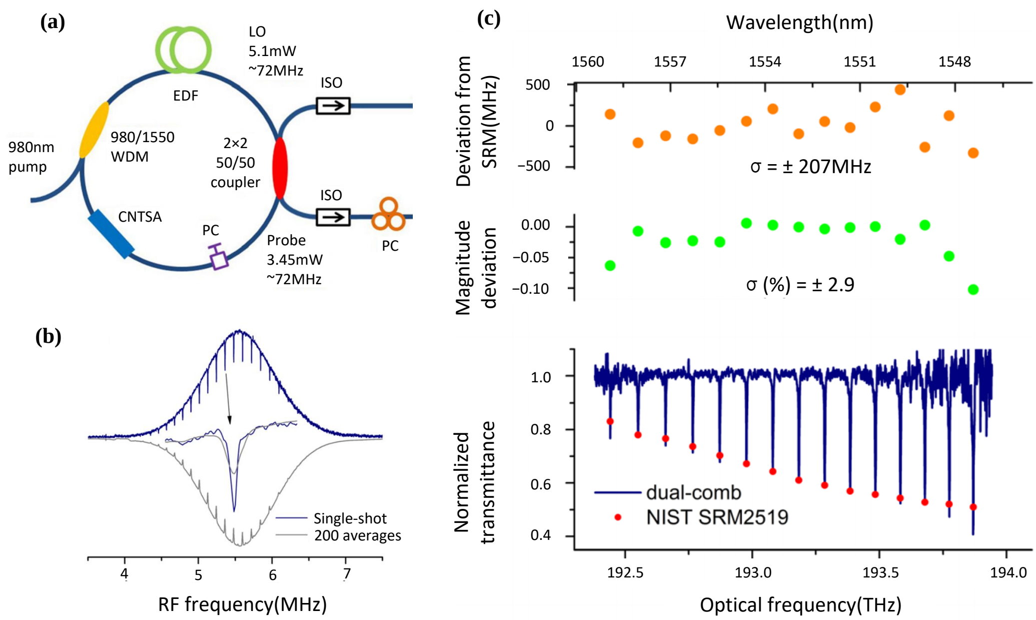

Figure 3. Experimental results of the DCS based on a bidirectional dual-comb laser. (**a**) Schematic diagram of the DCS system. (**b**) Absorption spectra of HCN calculated from single-shot (blue) and 200-times averaged (gray) interferograms, respectively. (**c**) Extracted absorption lines of 100 Torr, 16.5 cm HCN gas cell measured by proposed the DCS system and the deviations compared to the corresponding NIST SRM2519 data. Reproduced with permission [62]. Copyright 2016 authors, published by AIP Publishing.

In 2019, Satio et al. proposed an all-polarization-maintained bidirectional dual-comb fiber laser. The polarization-maintained structure effectively improved the long-term stability and repeatability of the dual-comb laser [82]. Nakajima et al. designed a high-coherence ultra-broadband bidirectional dual-comb fiber laser. Through nonlinear spectral broadening, two high-coherent ultra-broadband frequency combs were generated with a small repetition rate difference of 1.5 Hz. Thus, it allowed the measurable optical spectral bandwidth to attain ∼479 THz (∼3888 nm) [76]. In 2020, Lee et al. effectively improved the pulse energy of bidirectional dual combs by utilizing an all-normal dispersion laser based on nonlinear polarization rotation, where pulse energies of 1.56 nJ were far beyond the pulse energy limit of 50 pJ in the past [83]. In 2022, Galtier et al. firstly achieved measurement at the GHz resolution level by using a Kerr-lens mode-locked bidirectional Ti: sapphire ring laser cavity. The result is 2 orders of magnitude better than the previous report. The pulses were sufficient absolute and mutual coherence for 1.5-GHz resolution measurements [84].

3.2. Single-Cavity Dual Combs Based on Wavelength-Multiplexing

The multi-pulse operation can be generated by introducing a filter in the anomalous dispersion cavity due to the limitation of the soliton area theorem [85]. Dual-wavelength or even multi-wavelength mode-locking can be achieved by adjusting the cavity parameters owing to the periodic structure of sinusoidal filters. The multi-pulse of multi-wavelength mode-locking exhibits different repetition frequencies because of the distinct group velocities at different wavelengths, which can be regarded as wavelength-multiplexed dual combs.

In 2011, Zhao et al. firstly reported on wavelength-multiplexed dual combs in a dual-wavelength mode-locked fiber laser. The dual-wavelength operation was generated when the gains of erbium-doped fiber were similar at the two peaks of wavelengths. Thus, two mode-locked pulses with different repetition rates were achieved due to the group velocity dispersion [86]. In 2016, Zhao et al. demonstrated a DCS system based on the wavelength-multiplexed dual comb laser. Simple constant-clock sampling and data processing processes were used to achieve a spectral resolution of picometer level (1.5 pm) [61]. The DCS based on wavelength-multiplexing was then expanded to 1- and 2-μm band [87,88]. In general, the repetition rate difference of wavelength-multiplexed dual-comb systems is generally determined by the period of the filter. Mechanical filters were designed to adjust the repetition rate difference [89,90]. In general, mechanical filters were achieved by inserting a beam block into the grating compressor section. The length of the grating compressor can be dynamically adjusted by changing the effective width of the beam block, so that a controllable repetition rate difference was achieved. Besides, a thermally controlled Lyot filter composed of polarization-maintaining fiber (PMF) was investigated to achieve tunable operation of mode-locking in the dual-wavelength laser. The 25-nm tunable central wavelength and switch of single-wavelength and dual-wavelength operations were stably achieved by tuning the temperature of the Lyot filter [91].

Apart from the optimization of filters, novel saturable absorbers were employed to realize low-cost, high-output, and stable wavelength-multiplexed dual combs. In 2019, Zhao et al. demonstrated a dual-wavelength mode-locked laser by inserting multimode fibers between two single-mode fibers as a saturable absorber [92]. In 2021, Lin et al. applied carboxyl-functionalized graphene oxide as a saturable absorber in an erbium-doped laser (Figure 4a), which was simply manufactured and low-cost [93]. In order to overcome the ambiguity problem caused by the DCS, Li et al. proposed a multidimensional multiplexed approach to generate tri-comb and quad-comb systems, where wavelength- and polarization-multiplexed techniques were both utilized. The tri-comb system can eliminate physical delay stages in multidimensional coherent spectroscopy compared with the DCS [94].

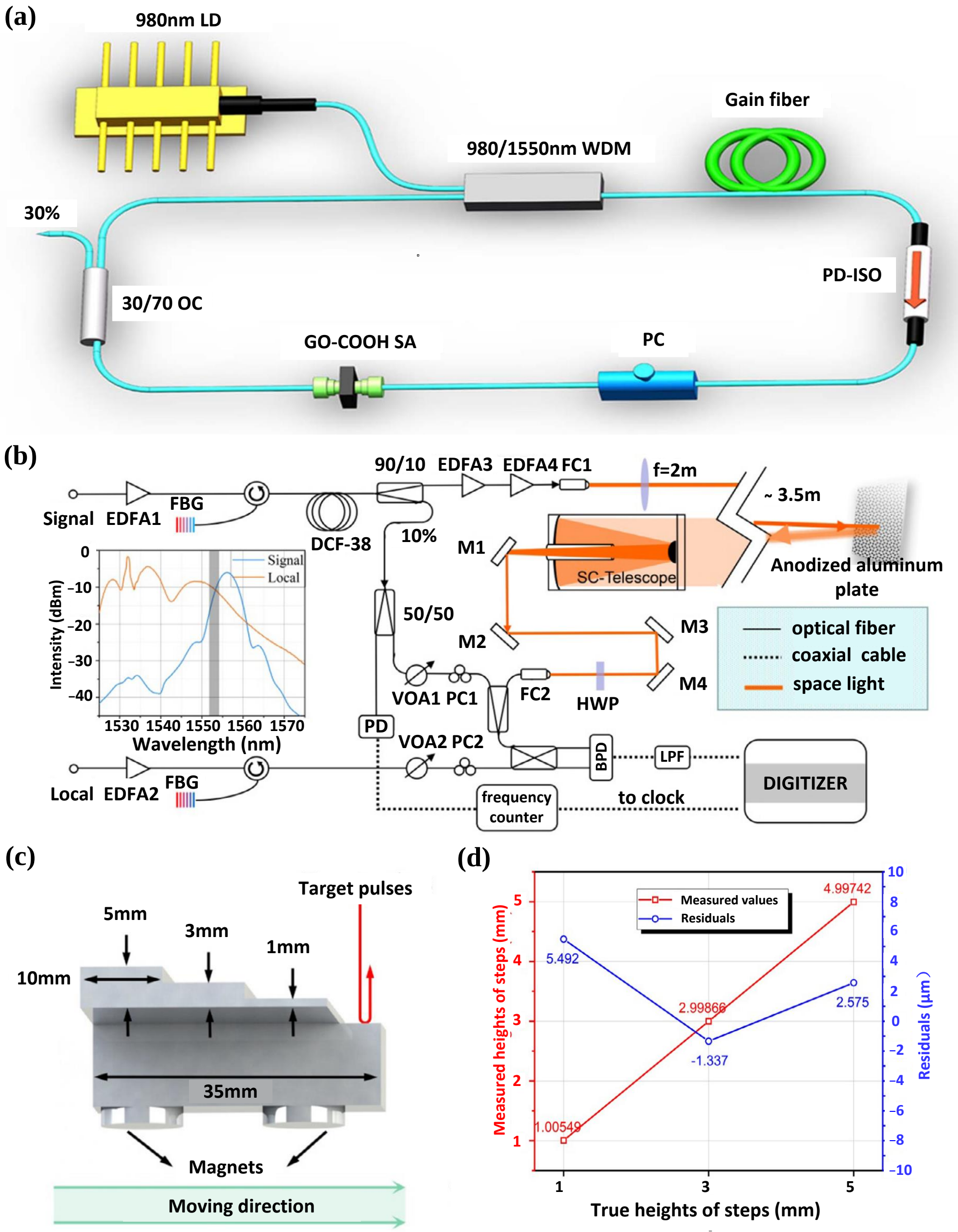

Figure 4. Experimental results of wavelength-multiplexed dual combs. (**a**) The schematic diagram of wavelength-multiplexed dual combs. Reproduced with permission [93]. Copyright 2021 Chinese Optics Letters. (**b**) The experimental setup of absolute distance measurement based on wavelength-multiplexed dual combs. (**c**) Top view of the gauge blocks being measured. (**d**) Measured heights and residuals of the gauge blocks. Reproduced with permission [65]. Copyright 2020 Elsevier.

Dual-comb system with a supercontinuum spectrum was achieved by using spread spectrum technology, which can cover more absorption lines of molecules. In 2021, Gu et al. compressed the output of a 1.5-μm dual-wavelength mode-locked laser. A dual-comb system with a broadband range of 1 to 1.75 μm was obtained by spectrally selected amplification, which had a lot of potential for dual-comb applications such as coherent anti-stokes Raman spectroscopy and mid-infrared differential frequency generation [95]. In 2019, Fellinger et al. proposed a dual-wavelength all-PMF fiber dual-comb laser for the first time. The stability of the dual-comb laser was improved due to the all-PMF fiber structure, which effectively resist environmental changes including temperature variations and slight perturbations [89]. In 2021, Guo et al. achieved self-starting dual combs in dual-wavelength all-PMF fiber lasers. Self-starting dual-wavelength mode-locking was achieved by the reflection-type PM-Lyot filter and nonlinear amplifying loop mirror [96]. Kelly sidebands contained in the conventional solitons may cause the wastage of energy and useful spectral range of the DCS. In 2022, Tao et al. investigated a sideband-free dual-comb system based on a dual-wavelength mode-locked fiber laser, where the polarization-maintaining Er-doped fiber performed not only the gain medium but also the Lyot filter together with a polarization controller. The Kelly sidebands were effectively suppressed by the nonlinear polarization rotation technique [97].

3.3. Single-Cavity Dual Combs Based on Polarization-Multiplexing

Single-cavity dual combs based on polarization-multiplexing mainly exploit the fiber birefringence caused by the asymmetry of the fiber. The refractive indices are different along the fast and slow axes of asymmetric fibers. Polarization-multiplexed dual combs with slightly different repetition rates can be obtained when the nonlinear interaction between the orthogonal polarization modes cannot compensate for the group velocity mismatch caused by fiber birefringence.

In 2017, Akosman et al. firstly proposed a polarization-multiplexed dual-comb system at 2-µm band. Two orthogonally polarized pulses were decomposed from the vector solitons by locking the polarization evolution frequency. The repetition rate difference between the two orthogonally polarized pulses was achieved owing to the birefringence caused by the asymmetry of single-mode fibers [98]. The birefringence of the PMF benefits the generation of stable dual combs in nearly orthogonal states of polarization. In 2018, Zhao et al. reported on a polarization-multiplexed dual-comb laser by introducing a section of PMF. The difference in repetition rates can be adjusted by tuning the intracavity polarization controller [99]. In 2019, Deng et al. proposed a linear wavelength-multiplexed dual-comb laser based on a semiconductor saturable absorption mirror to achieve mode-locking. An erbium-doped PMF oscillator in the cavity enabled mode-locked operations simultaneously in two cross-polarization axes. This system can be phase-locked without the need for an additional active frequency stabilization system [100]. Nakajima et al. firstly investigated an all-PMF polarization-multiplexed dual-comb system based on a nonlinear amplifying loop mirror. The all-PMF structure is more resistant to environmental disturbances, which facilitates the application of such dual combs in practical environments other than laboratories [101]. In 2020, Uyama et al. employed two 90-degree rotation splices in the all-PMF multiplexed dual-comb system to switch between fast and slow axes, which could balance the polarization-dependent loss and optimize the signal transmission quality [102]. Zhao et al. studied the dynamics of vector solitons in a polarization multiplexed dual-comb fiber laser by using the time-stretched dispersive Fourier transform technique [103]. The initiation process, build-up process, and vector-soliton collisions were observed and discussed experimentally and theoretically, which can guide the optimization of applications based on polarization-multiplexed dual combs.

In 2022, Hu et al. reported on a polarization-multiplexed dual-comb fiber laser with a tunable repetition rate difference from 12 Hz to 12 kHz, as shown in Figure 5a. The linear polarization mode dispersion enabled repetition rate difference at kHz level, while the repetition rate difference at the 10-Hz level resulted from the hybrid operation of the birefringence filter effect and nonlinear polarization evolution [104]. To date, the polarization-multiplexed dual combs at 1-µm band were commonly generated from solid-state lasers [105–107]. Solid-state lasers have a longer up-state lifetime, which allows the pulse to have higher pulse energy. The repetition rate difference of solid-state polarization-multiplexed dual combs commonly resulted from the 45°-cut birefringent crystal due to the non-common intracavity path and crystal dispersion.

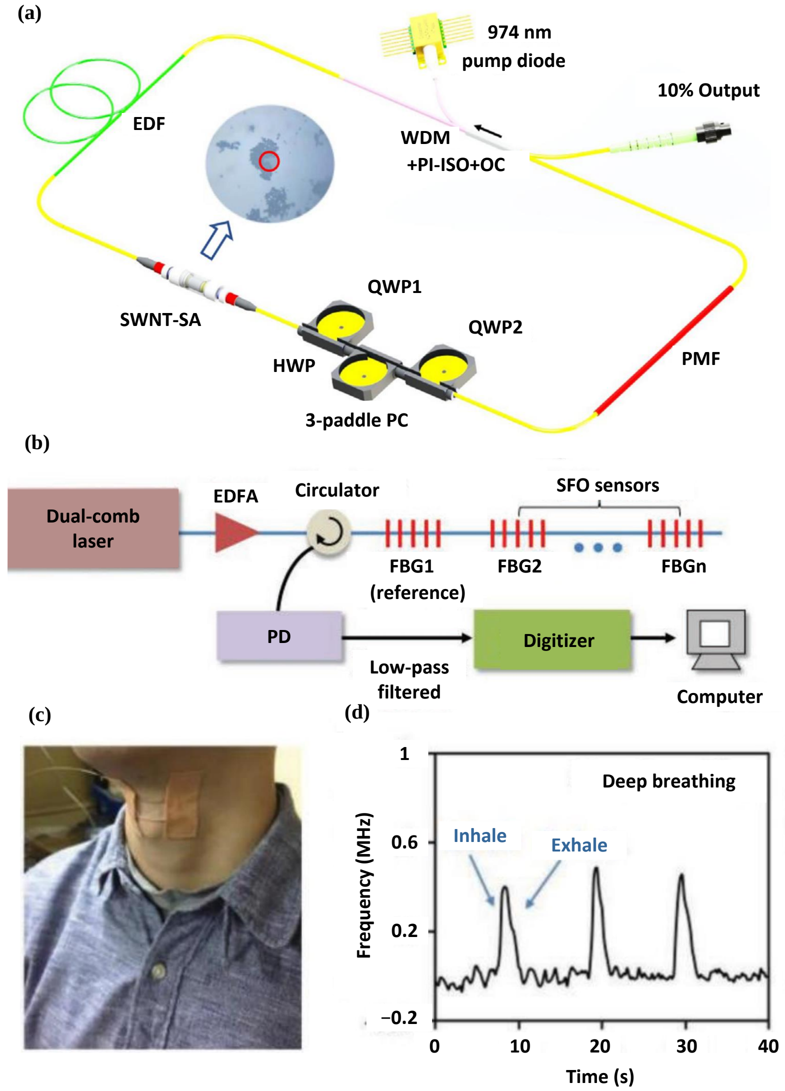

Figure 5. Device and application of laser based on polarization-multiplexing. (**a**) The setup of laser based on polarization-multiplexing. Reproduced with permission [104]. Copyright 2022 American Institute of Physics. (**b**) The experimental setup of wearable and skin-mountable fiber-optic strain sensors interrogated by a dual-comb fiber laser. (**c**) Profile display of the sensor attached to the volunteer's neck. (**d**) Response of the sensor to deep inhalations and exhalations. Reproduced with permission [108]. Copyright 2019 Wiley.

3.4. Single-Cavity Dual Combs Based on Space-Multiplexing

The non-shared cavity structures enable vast innovation of single-cavity dual combs. The different cavity lengths or gain mediums in the space-multiplexed dual combs allow for large tunable ranges of repetition rate and repetition rate difference, which is conducive to high-speed DCS.

In 2020, Zhao et al. firstly proposed a dual-color fiber laser based on space-multiplexing, where a single-mode-multimode-single-mode fiber structure was employed as the shared saturable absorber. Dual-color pulses with a stable repetition rate difference were generated from the Er- and Tm-doped laser cavities simultaneously, composed of space-multiplexed dual combs [109]. However, the non-shared section of space-multiplexed dual combs introduced disturbance due to the slow environmental drift. Thus, feedback loops were employed to reduce the frequency jitter.

In 2022, Pupeikis et al. achieved a space-multiplexed dual-comb laser, where a biprism on the surface was used for adjusting the repetition rate difference. A slow cross-correlationbased feedback loop was placed in the position of the biprism to obtain a stable dual-comb laser. The long-term stability of the dual-comb system was experimentally estimated to be 2.3×10^{-7} over 5 h [110].

4. Applications

The DCS based on single-cavity dual-comb lasers has been applied in enormous disciplines owing to the simple structure and low cost. Various applications based on single-cavity dual combs are presented in this section, including absorption spectroscopy, fiber sensing, distance measurement, combustion diagnostics, and coherent anti-Stokes Raman spectroscopy.

Spectroscopy is one of the most important application fields of single-cavity dual-comb systems. In 2016, Mwhravar et al. first employed a bidirectional mode-locked fiber laser at 1.5-µm band for absorption spectrum measurement. The dual-comb laser was relatively stable with an Allan deviation of 3×10^{8} in 1.28 ms. The precision of the bidirectional DCS was proved by measuring narrow absorption lines of HCN in the P-band. As shown in Figure 3b,c, the measured absorption lines had a deviation of ∼207 MHz from the NIST SRM2519 database [62]. In 2018, Olson et al. employed a 2-µm bidirectional mode-locked laser to measure the absorption of atmospheric water vapor over 945-GHz bandwidth [81]. Kayes et al. proposed a bidirectional mode-locked fiber laser at 2 µm. The dual-comb laser with 16-MHz repetition rate and 1.3-kHz repetition rate difference was employed to measure the absorption of ambient water vapor by the DCS at 1.9 µm [111]. There are various molecular fingerprints in the spectral region of 1.7–2.0 µm, including important industrial intermediates such as water vapor, methane, and carbon dioxide. Thus, it is necessary to broaden the wavelength coverage of the dual comb. In 2019, Chen et al. extended the wavelength coverage of a 1.5-µm wavelength-multiplexed dual-comb laser to 1.7 µm. The absorption spectrum of methane was measured by the DCS, which was completed in good agreement with HITRAN database [112]. Besides, novel techniques have also employed to assist in the measurement of absorption spectra, such as data processing and phase correction techniques. In 2019, Sterczewski et al. employed a 1.5-µm dual-comb laser based on polarization multiplexing to detect absorption spectrum of HCN. The repetition rate and repetition rate difference were 140 MHz and 3.2 kHz, respectively. An all-computational phase correction algorithm was employed. The absorption lines of HCN with narrow linewidths under low pressure were measured within 1.7 THz bandwidth, where the transmittance precision over a terahertz was better than 1% [113]. In 2020, Chen et al. utilized a wavelength-multiplexed dual-comb laser with the adaptive sampling method to measure the absorption spectrum of acetonitrile under low pressure. The dual combs had a repetition rate of 49 MHz and a repetition rate difference of 190 Hz. Doppler-limit-approaching absorption lines with narrow linewidths were first realized in such a low-repetition-rate dual-comb system by correcting the frequency drift with adaptive sampling method [114]. In 2022, Tian et al. demonstrated a dual-comb laser based on space-multiplexing, as shown in Figure 6a. The dual-comb laser at 1.5 µm was with 51-MHz repetition rate and 1.5-kHz repetition rate difference. Data post-processing and all-computational phase correction techniques were used to improve the long-term mutual coherence. The absorption spectrum of the HCN with 3-nm bandwidth was obtained, which agreed well with the HITRAN database as shown in Figure 6b,c [115].

The capability of single-cavity dual-comb systems in the DCS was also proved in fiber sensing. In general, the spectral shift of fiber grating sensors is a key parameter detected by dual-comb systems. In 2018, Guo et al. applied a bidirectional dual-comb laser to a fiber Bragg grating (FBG)-based multiplexed strain sensing system. The dual-comb laser was at 1.5-µm with 21-MHz repetition rate and 9-Hz repetition rate difference. The strain-induced spectral shift of the FBG sensors was precisely detected by the dual-comb system [66]. This fiber sensing technology already has practical applications in real life conditions. In 2019, Guo et al. employed polarization-multiplexed dual combs in a stretchable fiber optical strain sensor based on FBGs for the real-time monitoring of human activity, as shown in

Figure 5b. The sensor was attached to the volunteer's neck as shown in Figure 5c. The deep inhalations and exhalations reflected in shifts of Bragg wavelengths were further detected by the DCS, as shown in Figure 5d [108].

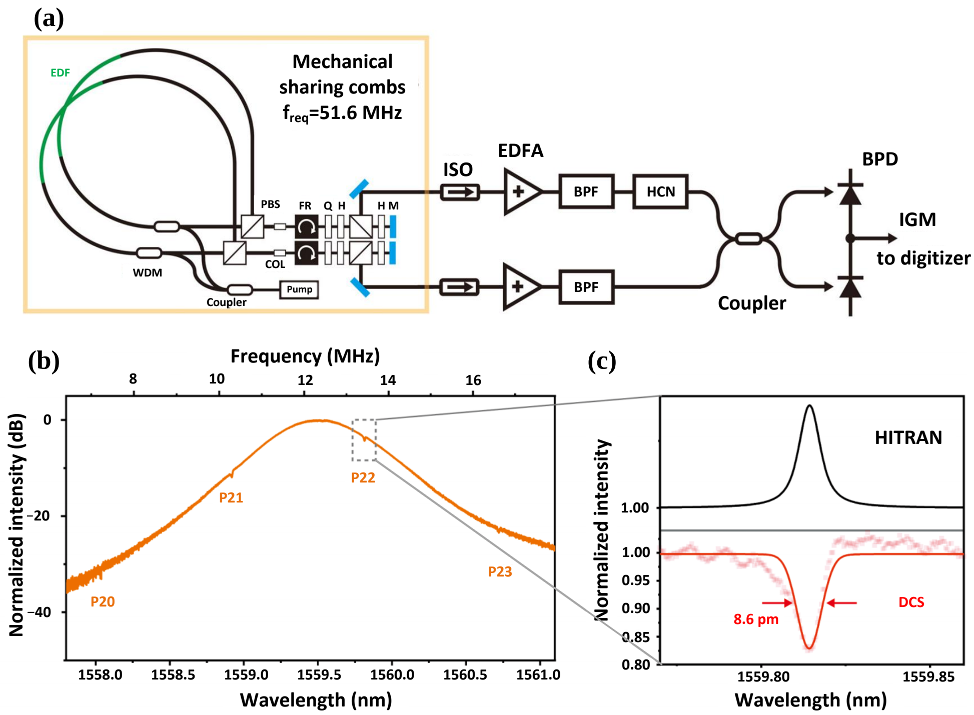

Figure 6. Experimental results of space-multiplexed dual combs. (**a**) The schematic diagram of space-multiplexed dual combs. (**b**) The absorption spectrum of HCN measured by the DCS. (**c**) The comparison between the measured P22 absorption line and the counterpart in the HITRAN database. Reproduced with permission [115]. Copyright 2022 American Institute of Physics.

In addition, single-cavity dual combs were used in the field of distance measurement, combustion diagnostics, and Terahertz spectroscopy. In 2020, Kieu et al. employed a 1.5-μm bidirectional mode-locked laser to coherent anti-Stokes Raman scattering. One comb was shifted to 1060 nm, used as the pump field, while the other comb at 1.5 μm was used as the Stokes field. The Raman spectra of multiple samples were observed in the C–H stretching window (2800 to 3100 cm^{-1}). The automatic scanning of the pump beam and Stokes beam were achieved, which greatly improved the excitation rate of the anti-Stokes signal [116]. In 2021, Hu et al. performed absolute distance measurement by using the DCS based on wavelength-multiplexing, as shown in Figure 4b. The output of free-running dual-comb system was extended to 1∼1.75 μm. This device could realize an accuracy of <10 μm, as shown in Figure 4c,d [65]. Nürnberg et al. firstly demonstrated a long-range distance measuring system with high resolution based on solid-state polarization-multiplexed dual combs. Two types of dual combs were employed in the laser ranging experiments, including a mode-locked integrated external cavity surface-emitting laser and a Yb:CaF_2 solid-state laser. The solid-state dual-comb laser performed higher resolution, while the mode-locked integrated external cavity surface-emitting laser can be sampled at a higher update rate. A resolution below 1 μm and a measurement range above 1 km could be anticipated by further optimization [64]. Xu et al. employed a wavelength-multiplexed dual-comb laser to non-intrusively collect the absorption spectrum of water and acetylene in a laminar premixed flame. Although the signal-to-noise ratio is smaller than that of phased-locked DCS, it is sufficient for most combustion reaction studies [117].

5. Conclusions and Perspectives

Due to their simple structure and high coherence, single-cavity dual combs have become attractive for DCS. Multiple methods have been developed to achieve single-cavity dual combs, including direction-multiplexing wavelength-multiplexing, polarization-multiplexing, and space-multiplexing. The single-cavity dual combs with overlapped spectra can be directly employed in spectral measurement, such as bidirectional and polarization-multiplexed dual combs [62,111,112].

The four methods each have their own strengths and weaknesses. As for bidirectional dual combs, the pulses output from opposite directions generally have overlapped spectra, which makes for a simple spectral analysis. However, the repetition rate difference is too small to achieve rapid measurement. In addition, the useful information may be submerged in the noise caused by the drift of repetition rates. Wavelength-multiplexed dual combs possess a large tunable range of repetition rate difference. However, the two combs at different center wavelengths need extra processes such as amplification and spectral spread to satisfy the requirements of applications. Dual-comb systems based on polarization-multiplexing have overlapped spectra and large repetition rate differences. Nevertheless, it is hard to control the repetition rate difference artificially. The non-common cavity structures of space-multiplexed dual combs are beneficial to realize the large repetition rate difference. However, the coherence might be reduced accordingly. Thus, the choice of dual-comb systems depends on the specific requirements of particular applications. Bidirectional and polarization-multiplexed dual combs are beneficial to simplify the spectroscopic measurements. Dual combs based on wavelength-multiplexing and space-multiplexing are suitable for fiber sensing and rapid measurements profiting from the large tunable range of repetition rate difference.

Single-cavity dual combs at 1-, 1.5-, and 2-µm bands have been widely reported [87,88,94]. A variety of important industrial intermediates, such as water vapor, carbon dioxide, and methane, are mainly located in the spectral region of 1.5–2.0 µm. Therefore, single-cavity dual-comb lasers at 1.5- and 2-µm bands were advantageous for species absorption spectrum measurements [81,112]. To date, the single-cavity dual combs at 1-µm were mostly achieved in solid-state lasers with higher output power [87,89,90], which have the potential for practical applications requiring high energy laser sources.

However, the limited repetition rate difference poses a significant challenge to improving the acquisition speed. Therefore, there is still a lot of room for improvement in single-cavity dual comb lasers. First, the tuning range of repetition rate difference can be further enlarged, which is not only beneficial for high-speed measurement but also reduces the disturbance caused by frequency jitter. Novel optical devices such as mechanical structures can be introduced in the laser cavity to realize the flexible adjustment of repetition rate difference [89,90] Second, the output power of all-fiber single-cavity dual combs may be insufficient for practical applications. However, the mutual coherence of single-cavity dual combs might be weakened due to additional amplifiers. Thus, solid-state and multimode-fiber-based lasers are compelling options for improving high-energy single-cavity dual combs [95–97,109]. Besides, the repetition rate difference is not fixed at each startup owing to the manually adjusted deviation of the laser state. Calibration algorithms and the intelligent control of mode-locking are important for supporting practical applications based on single-cavity dual comb lasers [118,119]. Moreover, the spectral range of single-cavity dual comb laser can be expanded to the mid-infrared region, in which the molecular absorption is stronger than that in the near-infrared [120]. Finally, single-cavity dual combs lasers combined with techniques such as Raman spectroscopy and coherent anti-Stokes Raman scattering can be used for spectral imaging in many practical applications [121].

Author Contributions: Conceptualization, B.F. and C.Z.; methodology, B.F. and C.Z.; software, P.O.; validation, C.Z., F.Q., P.O., H.S., S.H. and B.F.; formal analysis, C.Z., F.Q., P.O. and S.H.; investigation, F.Q.; resources, F.Q.; data curation, F.Q. and S.H.; writing—original draft preparation, C.Z., F.Q., P.O., H.S. and S.H.; writing—review and editing, C.Z.; visualization, F.Q., P.O. and S.H.; supervision, C.Z. and B.F.; project administration, C.Z. and B.F.; funding acquisition, B.F. All authors have read and agreed to the published version of the manuscript.

Funding: This research was funded by the National Natural Science Foundation of China (grants 62071016 and 62111530239), and the Fundamental Research Funds for the Central Universities.

Institutional Review Board Statement: Not applicable.

Informed Consent Statement: Not applicable.

Data Availability Statement: Not applicable.

Conflicts of Interest: The authors declare no conflict of interest.

References

1. Maiman, T. Stimulated optical radiation in ruby. *Nature* **1960**, *187*, 493–494. [CrossRef]
2. Hostetler, C.A.; Behrenfeld, M.J.; Hu, Y.; Hair, J.W.; Schulien, J.A. Spaceborne lidar in the study of marine systems. *Annu. Rev. Mar. Sci.* **2018**, *10*, 121–147. [CrossRef] [PubMed]
3. Li, N.; Ho, C.P.; Xue, J.; Lim, L.W.; Chen, G.; Fu, Y.H.; Lee, L.Y.T. A progress review on solid-state LiDAR and nanophotonics-based LiDAR sensors. *Laser Photonics Rev.* **2022**, *16*, 2100511. [CrossRef]
4. Palneedi, H.; Park, J.H.; Maurya, D.; Peddigari, M.; Hwang, G.T.; Annapureddy, V.; Kim, J.W.; Choi, J.J.; Hahn, B.D.; Priya, S.; et al. Laser irradiation of metal oxide films and nanostructures: applications and advances. *Adv. Mater.* **2018**, *30*, 1705148. [CrossRef]
5. Dutta Majumdar, J.; Manna, I. Laser material processing. *Int. Mater. Rev.* **2011**, *56*, 341–388. [CrossRef]
6. Udem, T.; Holzwarth, R.; Hänsch, T.W. Optical frequency metrology. *Nature* **2002**, *416*, 233–237. [CrossRef]
7. Kandula, D.Z.; Gohle, C.; Pinkert, T.J.; Ubachs, W.; Eikema, K.S. Extreme ultraviolet frequency comb metrology. *Phys. Rev. Lett.* **2010**, *105*, 063001. [CrossRef]
8. Aiello, R.; Di Sarno, V.; Delli Santi, M.G.; De Rosa, M.; Ricciardi, I.; De Natale, P.; Santamaria, L.; Giusfredi, G.; Maddaloni, P. Absolute frequency metrology of buffer-gas-cooled molecular spectra at 1 kHz accuracy level. *Nat. Commun.* **2022**, *13*, 7016. [CrossRef]
9. Pupeza, I.; Zhang, C.; Hogner, M.; Ye, J. Extreme-ultraviolet frequency combs for precision metrology and attosecond science. *Nat. Photonics* **2021**, *15*, 175–186. [CrossRef]
10. Grelu, P.; Akhmediev, N. Dissipative solitons for mode-locked lasers. *Nat. Photonics* **2012**, *6*, 84–92. [CrossRef]
11. Sun, Z.; Hasan, T.; Torrisi, F.; Popa, D.; Privitera, G.; Wang, F.; Bonaccorso, F.; Basko, D.M.; Ferrari, A.C. Graphene mode-locked ultrafast laser. *ACS Nano* **2010**, *4*, 803–810. [CrossRef] [PubMed]
12. Fu, B.; Sun, J.; Wang, G.; Shang, C.; Ma, Y.; Ma, J.; Xu, L.; Scardaci, V. Solution-processed two-dimensional materials for ultrafast fiber lasers. *Nanophotonics* **2020**, *9*, 2169–2189. [CrossRef]
13. Zhang, M.; Wu, Q.; Zhang, F.; Chen, L.; Jin, X.; Hu, Y.; Zheng, Z.; Zhang, H. 2D black phosphorus saturable absorbers for ultrafast photonics. *Adv. Opt. Mater.* **2019**, *7*, 1800224. [CrossRef]
14. Zhao, X.; Jin, H.; Liu, J.; Chao, J.; Liu, T.; Zhang, H.; Wang, G.; Lyu, W.; Wageh, S.; Al-Hartomy, O.A.; et al. Integration and applications of nanomaterials for ultrafast photonics. *Laser Photonics Rev.* **2022**, *16*, 2200386. [CrossRef]
15. Fu, B.; Sun, J.; Cheng, Y.; Ouyang, H.; Compagnini, G.; Yin, P.; Wei, S.; Li, S.; Li, D.; Scardaci, V.; et al. Recent progress on metal-based nanomaterials: fabrications, optical properties, and applications in ultrafast photonics. *Adv. Funct. Mater.* **2021**, *31*, 2107363. [CrossRef]
16. Wang, G.; Liu, T.; Chao, J.; Jin, H.; Liu, J.; Zhang, H.; Lyu, W.; Yin, P.; Al-Ghamdi, A.; Wageh, S.; et al. Recent advances and challenges in ultrafast photonics enabled by metal nanomaterials. *Adv. Opt. Mater.* **2022**, *10*, 2200443. [CrossRef]
17. Fu, B.; Sun, J.; Wang, C.; Shang, C.; Xu, L.; Li, J.; Zhang, H. MXenes: Synthesis, optical properties, and applications in ultrafast photonics. *Small* **2021**, *17*, 2006054. [CrossRef]
18. Cheng, Y.; Lyu, W.; Wang, Z.; Ouyang, H.; Zhang, A.; Sun, J.; Yang, T.; Fu, B.; He, B. MXenes: Synthesis, incorporation, and applications in ultrafast lasers. *Nanotechnology* **2021**, *32*, 392003. [CrossRef]
19. Zhang, A.; Wang, Z.; Ouyang, H.; Lyu, W.; Sun, J.; Cheng, Y.; Fu, B. Recent progress of two-dimensional materials for ultrafast photonics. *Nanomaterials* **2021**, *11*, 1778. [CrossRef]
20. Weber, R.; Graf, T.; Berger, P.; Onuseit, V.; Wiedenmann, M.; Freitag, C.; Feuer, A. Heat accumulation during pulsed laser materials processing. *Opt. Express* **2014**, *22*, 11312–11324. [CrossRef]
21. Sugioka, K.; Cheng, Y. Ultrafast lasers—Reliable tools for advanced materials processing. *Light. Sci. Appl.* **2014**, *3*, e149. [CrossRef]
22. Korte, F.; Nolte, S.; Chichkov, B.; Bauer, T.; Kamlage, G.; Wagner, T.; Fallnich, C.; Welling, H. Far-field and near-field material processing with femtosecond laser pulses. *Appl. Phys. -Mater. Sci. Process.* **1999**, *69*, S7–S11. [CrossRef]

23. Varnavski, O.; Goodson, T., III. Two-photon fluorescence microscopy at extremely low excitation intensity: The power of quantum correlations. *J. Am. Chem. Soc.* **2020**, *142*, 12966–12975. [CrossRef] [PubMed]
24. Vogel, A.; Venugopalan, V. Mechanisms of pulsed laser ablation of biological tissues. *Chem. Rev.* **2003**, *103*, 577–644. [CrossRef]
25. Li, J.; Shang, C.; Rong, Y.; Sun, J.; Cheng, Y.; He, B.; Wang, Z.; Li, M.; Ma, J.; Fu, B.; et al. Review on laser Technology in intravascular imaging and treatment. *Aging Dis.* **2022**, *13*, 246. [CrossRef] [PubMed]
26. Haus, H.A. Mode-locking of lasers. *IEEE J. Sel. Top. Quantum Electron.* **2000**, *6*, 1173–1185. [CrossRef]
27. Essen, L.; Parry, J.V.L. An Atomic Standard of Frequency and Time Interval: A Cæsium Resonator. *Nature* **1955**, *176*, 280–282. [CrossRef]
28. Hall, J.L. Nobel Lecture: Defining and measuring optical frequencies. *Rev. Mod. Phys.* **2006**, *78*, 1279. [CrossRef]
29. Hänsch, T.W. Nobel lecture: passion for precision. *Rev. Mod. Phys.* **2006**, *78*, 1297. [CrossRef]
30. Diddams, S.A.; Udem, T.; Bergquist, J.; Curtis, E.; Drullinger, R.; Hollberg, L.; Itano, W.M.; Lee, W.; Oates, C.; Vogel, K.; et al. An optical clock based on a single trapped 199Hg+ ion. *Science* **2001**, *293*, 825–828. [CrossRef]
31. Rosenband, T.; Hume, D.; Schmidt, P.; Chou, C.W.; Brusch, A.; Lorini, L.; Oskay, W.; Drullinger, R.E.; Fortier, T.M.; Stalnaker, J.E.; et al. Frequency ratio of Al+ and Hg+ single-ion optical clocks; metrology at the 17th decimal place. *Science* **2008**, *319*, 1808–1812. [CrossRef]
32. Trocha, P.; Karpov, M.; Ganin, D.; Pfeiffer, M.H.; Kordts, A.; Wolf, S.; Krockenberger, J.; Marin-Palomo, P.; Weimann, C.; Randel, S.; et al. Ultrafast optical ranging using microresonator soliton frequency combs. *Science* **2018**, *359*, 887–891. [CrossRef]
33. Coddington, I.; Swann, W.C.; Nenadovic, L.; Newbury, N.R. Rapid and precise absolute distance measurements at long range. *Nat. Photonics* **2009**, *3*, 351–356. [CrossRef]
34. Xu, X.; Zhang, Z.; Zhang, H.; Zhao, H.; Xia, W.; He, M.; Li, J.; Zhai, J.; Wu, H. Long distance measurement by dynamic optical frequency comb. *Opt. Express* **2020**, *28*, 4398–4411. [CrossRef] [PubMed]
35. Kuse, N.; Fermann, M.E. Frequency-modulated comb LIDAR. *APL Photonics* **2019**, *4*, 106105. [CrossRef]
36. Steinmetz, T.; Wilken, T.; Araujo-Hauck, C.; Holzwarth, R.; Hansch, T.W.; Pasquini, L.; Manescau, A.; D'odorico, S.; Murphy, M.T.; Kentischer, T.; et al. Laser frequency combs for astronomical observations. *Science* **2008**, *321*, 1335–1337. [CrossRef] [PubMed]
37. Diddams, S.A.; Hollberg, L.; Mbele, V. Molecular fingerprinting with the resolved modes of a femtosecond laser frequency comb. *Nature* **2007**, *445*, 627–630. [CrossRef] [PubMed]
38. Gohle, C.; Stein, B.; Schliesser, A.; Udem, T.; Hänsch, T.W. Frequency comb vernier spectroscopy for broadband, high-resolution, high-sensitivity absorption and dispersion spectra. *Phys. Rev. Lett.* **2007**, *99*, 263902. [CrossRef] [PubMed]
39. Maslowski, P.; Lee, K.F.; Johansson, A.C.; Khodabakhsh, A.; Kowzan, G.; Rutkowski, L.; Mills, A.A.; Mohr, C.; Jiang, J.; Fermann, M.E.; et al. Surpassing the path-limited resolution of Fourier-transform spectrometry with frequency combs. *Phys. Rev. A* **2016**, *93*, 021802. [CrossRef]
40. Schiller, S. Spectrometry with frequency combs. *Opt. Lett.* **2002**, *27*, 766–768. [CrossRef]
41. Keilmann, F.; Gohle, C.; Holzwarth, R. Time-domain mid-infrared frequency-comb spectrometer. *Opt. Lett.* **2004**, *29*, 1542–1544. [CrossRef]
42. Rieker, G.B.; Giorgetta, F.R.; Swann, W.C.; Kofler, J.; Zolot, A.M.; Sinclair, L.C.; Baumann, E.; Cromer, C.; Petron, G.; Sweeney, C.; et al. Frequency-comb-based remote sensing of greenhouse gases over kilometer air paths. *Optica* **2014**, *1*, 290–298. [CrossRef]
43. Fu, B.; Zhang, C.; Lyu, W.; Sun, J.; Shang, C.; Cheng, Y.; Xu, L. Recent progress on laser absorption spectroscopy for determination of gaseous chemical species. *Appl. Spectrosc. Rev.* **2022**, *57*, 112–152. [CrossRef]
44. Zhu, F.; Bicer, A.; Askar, R.; Bounds, J.; Kolomenskii, A.; Kelessides, V.; Amani, M.; Schuessler, H. Mid-infrared dual frequency comb spectroscopy based on fiber lasers for the detection of methane in ambient air. *Laser Phys. Lett.* **2015**, *12*, 095701. [CrossRef]
45. Yu, H.; Zhou, Q.; Li, X.; Wang, X.; Wang, X.; Ni, K. Improving resolution of dual-comb gas detection using periodic spectrum alignment method. *Sensors* **2021**, *21*, 903. [CrossRef] [PubMed]
46. Godbout, M.; Deschênes, J.D.; Genest, J. Spectrally resolved laser ranging with frequency combs. *Opt. Express* **2010**, *18*, 15981–15989. [CrossRef] [PubMed]
47. Boudreau, S.; Levasseur, S.; Perilla, C.; Roy, S.; Genest, J. Chemical detection with hyperspectral lidar using dual frequency combs. *Opt. Express* **2013**, *21*, 7411–7418. [CrossRef]
48. LI, R.; Ren, X.; Han, B.; Yan, M.; Huang, K.; Liang, Y.; Ge, J.; Zeng, H. Ultra-rapid dual-comb ranging with an extended non-ambiguity range. *Opt. Lett.* **2022**, *47*, 5309–5312. [CrossRef]
49. Liu, Y.; Xia, W.; He, M.; Cao, S.; Miao, D.; Lin, B.; Xie, J.; Yang, W.; Li, J. Experimental realization and characterization of a two–color dual–comb system for practical large–scale absolute distance measurements. *Opt. Lasers Eng.* **2022**, *151*, 106900. [CrossRef]
50. Ideguchi, T.; Holzner, S.; Bernhardt, B.; Guelachvili, G.; Picqué, N.; Hänsch, T.W. Coherent Raman spectro-imaging with laser frequency combs. *Nature* **2013**, *502*, 355–358. [CrossRef]
51. Ideguchi, T.; Bernhardt, B.; Guelachvili, G.; Hänsch, T.W.; Picqué, N. Raman-induced Kerr-effect dual-comb spectroscopy. *Opt. Lett.* **2012**, *37*, 4498–4500. [CrossRef]
52. Thorpe, M.J.; Balslev-Clausen, D.; Kirchner, M.S.; Ye, J. Cavity-enhanced optical frequency comb spectroscopy: Application to human breath analysis. *Opt. Express* **2008**, *16*, 2387–2397. [CrossRef] [PubMed]
53. Martin-Mateos, P.; Ullah Khan, F.; Elias Bonilla-Manrique, O. Direct hyperspectral dual-comb imaging. *Optica* **2020**, *7*, 199–202. [CrossRef]

54. Vicentini, E.; Wang, Z.; Van Gasse, K.; Hansch, T.W.; Picque, N. Dual-comb hyperspectral digital holography. *Nat. Photonics* **2021**, *15*, 890–894. [CrossRef]
55. Wang, Q.; Wang, Z.; Zhang, H.; Jiang, S.; Wang, Y.; Jin, W.; Ren, W. Dual-comb photothermal spectroscopy. *Nat. Commun.* **2022**, *13*, 2181. [CrossRef] [PubMed]
56. Friedlein, J.T.; Baumann, E.; Briggman, K.A.; Colacion, G.M.; Giorgetta, F.R.; Goldfain, A.M.; Herman, D.I.; Hoenig, E.V.; Hwang, J.; Newbury, N.R.; et al. Dual-comb photoacoustic spectroscopy. *Nat. Commun.* **2020**, *11*, 3152. [CrossRef]
57. Wildi, T.; Voumard, T.; Brasch, V.; Yilmaz, G.; Herr, T. Photo-acoustic dual-frequency comb spectroscopy. *Nat. Commun.* **2020**, *11*, 4146. [CrossRef]
58. Millot, G.; Pitois, S.; Yan, M.; Hovhannisyan, T.; Bendahmane, A.; Hänsch, T.W.; Picqué, N. Frequency-agile dual-comb spectroscopy. *Nat. Photonics* **2016**, *10*, 27–30. [CrossRef]
59. Coddington, I.; Swann, W.C.; Newbury, N.R. Coherent multiheterodyne spectroscopy using stabilized optical frequency combs. *Phys. Rev. Lett.* **2008**, *100*, 013902. [CrossRef]
60. Suh, M.G.; Yang, Q.F.; Yang, K.Y.; Yi, X.; Vahala, K.J. Microresonator soliton dual-comb spectroscopy. *Science* **2016**, *354*, 600–603. [CrossRef]
61. Zhao, X.; Hu, G.; Zhao, B.; Li, C.; Pan, Y.; Liu, Y.; Yasui, T.; Zheng, Z. Picometer-resolution dual-comb spectroscopy with a free-running fiber laser. *Opt. Express* **2016**, *24*, 21833–21845. [CrossRef] [PubMed]
62. Mehravar, S.; Norwood, R.A.; Peyghambarian, N.; Kieu, K. Real-time dual-comb spectroscopy with a free-running bidirectionally mode-locked fiber laser. *Appl. Phys. Lett.* **2016**, *108*, 231104. [CrossRef]
63. Lin, B.; Zhao, X.; He, M.; Pan, Y.; Chen, J.; Cao, S.; Lin, Y.; Wang, Q.; Zheng, Z.; Fang, Z. Dual-comb absolute distance measurement based on a dual-wavelength passively mode-locked laser. *IEEE Photonics J.* **2017**, *9*, 1–8. [CrossRef]
64. Nurnberg, J.; Willenberg, B.; Phillips, C.R.; Keller, U. Dual-comb ranging with frequency combs from single cavity free-running laser oscillators. *Opt. Express* **2021**, *29*, 24910–24918. [CrossRef]
65. Hu, D.; Wu, Z.; Cao, H.; Shi, Y.; Li, R.; Tian, H.; Song, Y.; Hu, M. Dual-comb absolute distance measurement of non-cooperative targets with a single free-running mode-locked fiber laser. *Opt. Commun.* **2021**, *482*, 126566. [CrossRef]
66. Guo, J.; Ding, Y.; Xiao, X.; Kong, L.; Yang, C. Multiplexed static FBG strain sensors by dual-comb spectroscopy with a free running fiber laser. *Opt. Express* **2018**, *26*, 16147–16154. [CrossRef] [PubMed]
67. Ye, J.; Cundiff, S.T. *Femtosecond Optical Frequency Comb: Principle, Operation and Applications*; Springer Science & Business Media: New York, NY, USA, 2005.
68. Kieu, K.; Mansuripur, M. All-fiber bidirectional passively mode-locked ring laser. *Opt. Lett.* **2008**, *33*, 64–66. [CrossRef]
69. Cui, Y.; Liu, X. Graphene and nanotube mode-locked fiber laser emitting dissipative and conventional solitons. *Opt. Express* **2013**, *21*, 18969–18974. [CrossRef] [PubMed]
70. Zeng, C.; Liu, X.; Yun, L. Bidirectional fiber soliton laser mode-locked by single-wall carbon nanotubes. *Opt. Express* **2013**, *21*, 18937–18942. [CrossRef]
71. Yao, X. Generation of bidirectional stretched pulses in a nanotube-mode-locked fiber laser. *Appl. Opt.* **2014**, *53*, 27–31. [CrossRef]
72. Mamidala, V.; Woodward, R.; Yang, Y.; Liu, H.; Chow, K. Graphene-based passively mode-locked bidirectional fiber ring laser. *Opt. Express* **2014**, *22*, 4539–4546. [CrossRef]
73. Zhao, X.; Zheng, Z.; Liu, Y.; Hu, G.; Liu, J. Dual-wavelength, bidirectional single-wall carbon nanotube mode-locked fiber laser. *IEEE Photonics Technol. Lett.* **2014**, *26*, 1722–1725. [CrossRef]
74. Yang, Q.F.; Yi, X.; Yang, K.Y.; Vahala, K. Counter-propagating solitons in microresonators. *Nat. Photonics* **2017**, *11*, 560–564. [CrossRef]
75. Yang, R.; Sun, H.; Guo, J.; Fu, H.; Yang, H.; Hu, P.; Fan, Z.; Tan, J. Dual-comb generation from a dual-ring hybrid mode-locked fiber laser. In Proceedings of the Tenth International Symposium on Precision Engineering Measurements and Instrumentation, Kunming, China, 7 March 2019, Volume 11053, pp. 546–551.
76. Nakajima, Y.; Hata, Y.; Minoshima, K. High-coherence ultra-broadband bidirectional dual-comb fiber laser. *Opt. Express* **2019**, *27*, 5931–5944. [CrossRef]
77. Yang, K.; Li, T.J.; Li, X.D.; Chen, J.X.; Liu, M.; Cui, H.; Luo, A.P.; Xu, W.C.; Luo, Z.C. Mutually induced soliton polarization instability in a bidirectional ultrafast fiber laser. *Opt. Lett.* **2021**, *46*, 4848–4851. [CrossRef] [PubMed]
78. Bauer, C.; Camenzind, S.; Pupeikis, J.; Willenberg, B.; Phillips, C.; Keller, U. Dual-comb optical parametric oscillator in the mid-infrared based on a single free-running cavity. *Opt. Express* **2022**, *30*, 19904–19921. [CrossRef] [PubMed]
79. Lin, J.; Dong, Z.; Dong, T.; Ma, X.; Dai, C.; Yao, P.; Gu, C.; Xu, L. Bidirectional mode-locked fiber laser based on nonlinear multimode interference. *Opt. Laser Technol.* **2022**, *154*, 108269. [CrossRef]
80. Ouyang, C.; Shum, P.; Wu, K.; Wong, J.H.; Lam, H.Q.; Aditya, S. Bidirectional passively mode-locked soliton fiber laser with a four-port circulator. *Opt. Lett.* **2011**, *36*, 2089–2091. [CrossRef] [PubMed]
81. Olson, J.; Ou, Y.; Azarm, A.; Kieu, K. Bi-directional mode-locked thulium fiber laser as a single-cavity dual-comb source. *IEEE Photonics Technol. Lett.* **2018**, *30*, 1772–1775. [CrossRef]
82. Saito, S.; Yamanaka, M.; Sakakibara, Y.; Omoda, E.; Kataura, H.; Nishizawa, N. All-polarization-maintaining Er-doped dual comb fiber laser using single-wall carbon nanotubes. *Opt. Express* **2019**, *27*, 17868–17875. [CrossRef]
83. Li, B.; Xing, J.; Kwon, D.; Xie, Y.; Prakash, N.; Kim, J.; Huang, S.W. Bidirectional mode-locked all-normal dispersion fiber laser. *Optica* **2020**, *7*, 961–964. [CrossRef]

84. Galtier, S.; Pivard, C.; Morville, J.; Rairoux, P. High-resolution dual comb spectroscopy using a free-running, bidirectional ring titanium sapphire laser. *Opt. Express* **2022**, *30*, 21148–21158. [CrossRef]
85. Nelson, L.E.; Jones, D.; Tamura, K.; Haus, H.A.; Ippen, E. Ultrashort-pulse fiber ring lasers. *Appl. Phys. Lasers Opt.* **1997**, *65*, 277–294. [CrossRef]
86. Zhao, X.; Zheng, Z.; Liu, L.; Liu, Y.; Jiang, Y.; Yang, X.; Zhu, J. Switchable, dual-wavelength passively mode-locked ultrafast fiber laser based on a single-wall carbon nanotube modelocker and intracavity loss tuning. *Opt. Express* **2011**, *19*, 1168–1173. [CrossRef] [PubMed]
87. Huang, S.; Wang, Y.; Yan, P.; Zhao, J.; Li, H.; Lin, R. Tunable and switchable multi-wavelength dissipative soliton generation in a graphene oxide mode-locked Yb-doped fiber laser. *Opt. Express* **2014**, *22*, 11417–11426. [CrossRef]
88. Liao, R.; Song, Y.; Liu, W.; Shi, H.; Chai, L.; Hu, M. Dual-comb spectroscopy with a single free-running thulium-doped fiber laser. *Opt. Express* **2018**, *26*, 11046–11054. [CrossRef]
89. Fellinger, J.; Mayer, A.S.; Winkler, G.; Grosinger, W.; Truong, G.W.; Droste, S.; Li, C.; Heyl, C.M.; Hartl, I.; Heckl, O.H. Tunable dual-comb from an all-polarization-maintaining single-cavity dual-color Yb: fiber laser. *Opt. Express* **2019**, *27*, 28062–28074. [CrossRef] [PubMed]
90. Fellinger, J.; Winkler, G.; Mayer, A.S.; Steidle, L.R.; Heckl, O.H. Tunable dual-color operation of Yb: fiber laser via mechanical spectral subdivision. *Opt. Express* **2019**, *27*, 5478–5486. [CrossRef]
91. Sun, X.; Zhu, Y.; Jin, L.; Yamashita, S.; Set, S.Y. Polarization-maintaining all-fiber tunable mode-locked laser based on a thermally controlled Lyot filter. *Opt. Lett.* **2022**, *47*, 4913–4916. [CrossRef] [PubMed]
92. Zhao, K.; Jia, H.; Wang, P.; Guo, J.; Xiao, X.; Yang, C. Free-running dual-comb fiber laser mode-locked by nonlinear multimode interference. *Opt. Lett.* **2019**, *44*, 4323–4326. [CrossRef]
93. Lin, Q.; Yan, L.; Song, Y.; Jia, X.; Feng, X.; Hou, L.; Bai, J. Switchable single-and dual-wavelength femtosecond mode-locked Er-doped fiber laser based on carboxyl-functionalized graphene oxide saturable absorber. *Chin. Opt. Lett.* **2021**, *19*, 111405. [CrossRef]
94. Li, T.; Zhao, X.; Chen, J.; Li, Q.; Zheng, Z. Tri-Comb and Quad-Comb Generation Based on a Multi-Dimensional Multiplexed Mode-Locked Laser. *J. Light. Technol.* **2019**, *37*, 5178–5184. [CrossRef]
95. Gu, X.; Chen, H.; Li, Y.; Cao, X.; Wang, C.; Liu, Y. Ultrashort pulse duration and broadband dual-comb laser system based on a free-running passively mode-locked Er-fiber oscillator. *Laser Phys. Lett.* **2021**, *18*, 125101. [CrossRef]
96. Guo, Z.; Liu, T.; Peng, J.; Zhu, Y.; Zeng, H. Self-started dual-wavelength mode-locking with well-controlled repetition rate difference. *J. Light. Technol.* **2021**, *39*, 3575–3581. [CrossRef]
97. Tao, J.; Fang, Y.; Song, Y.; Song, P.; Hou, L.; Lu, B.; Lin, Q.; Bai, J. Sideband-free tunable and switchable dual-wavelength mode-locked fiber laser based on the Lyot filter and spontaneous radiation peaks. *Opt. Express* **2022**, *30*, 17465–17475. [CrossRef]
98. Akosman, A.E.; Sander, M.Y. Dual comb generation from a mode-locked fiber laser with orthogonally polarized interlaced pulses. *Opt. Express* **2017**, *25*, 18592–18602. [CrossRef]
99. Zhao, X.; Li, T.; Liu, Y.; Li, Q.; Zheng, Z. Polarization-multiplexed, dual-comb all-fiber mode-locked laser. *Photonics Res.* **2018**, *6*, 853–857. [CrossRef]
100. Deng, Z.; Liu, Y.; Ouyang, C.; Zhang, W.; Wang, C.; Li, W. Mutually coherent dual-comb source generated from a free-running linear fiber laser. *Results Phys.* **2019**, *14*, 102364. [CrossRef]
101. Nakajima, Y.; Hata, Y.; Minoshima, K. All-polarization-maintaining, polarization-multiplexed, dual-comb fiber laser with a nonlinear amplifying loop mirror. *Opt. Express* **2019**, *27*, 14648–14656. [CrossRef]
102. Uyama, K.; Shirahata, T.; Jin, L.; Set, S.Y.; Yamashita, S. All-PM dual-comb fiber ring laser using CNT-SA. In Proceedings of the CLEO: Science and Innovations. Optical Society of America, Washington, DC, USA, 10–15 May 2020; p. SW4R–2.
103. Zhao, K.; Gao, C.; Xiao, X.; Yang, C. Buildup dynamics of asynchronous vector solitons in a polarization-multiplexed dual-comb fiber laser. *Opt. Lett.* **2020**, *45*, 4040–4043. [CrossRef]
104. Hu, G.; Zhu, L.; Sun, G.; Lu, L.; You, R.; Liu, Y.; He, W.; Dong, M. Spectral overlapping single-cavity dual-comb fiber laser with well-controlled repetition rate difference. *Appl. Phys. Lett.* **2022**, *121*, 091101. [CrossRef]
105. Willenberg, B.; Pupeikis, J.; Krüger, L.M.; Koch, F.; Phillips, C.R.; Keller, U. Femtosecond dual-comb Yb: CaF 2 laser from a single free-running polarization-multiplexed cavity for optical sampling applications. *Opt. Express* **2020**, *28*, 30275–30288. [CrossRef]
106. Kowalczyk, M.; Sterczewski, Ł.; Zhang, X.; Petrov, V.; Wang, Z.; Sotor, J. Dual-comb femtosecond solid-state laser with inherent polarization-multiplexing. *Laser Photonics Rev.* **2021**, *15*, 2000441. [CrossRef]
107. Koenen, D.; Willenberg, B.; Pupeikis, J.; Camenzind, S.; Phillips, C.; Keller, U. Single-cavity dual-comb Yb: CaF2 laser pumped by a single-mode laser diode. In *CLEO: Science and Innovations*; Optica Publishing Group: San Diego, CA, USA, 2021; p. STu2E–4.
108. Guo, J.; Zhao, K.; Zhou, B.; Ning, W.; Jiang, K.; Yang, C.; Kong, L.; Dai, Q. Wearable and skin-mountable fiber-optic strain sensors interrogated by a free-running, dual-comb fiber laser. *Adv. Opt. Mater.* **2019**, *7*, 1900086. [CrossRef]
109. Zhao, K.; Li, Y.; Xiao, X.; Yang, C. Nonlinear multimode interference-based dual-color mode-locked fiber laser. *Opt. Lett.* **2020**, *45*, 1655–1658. [CrossRef] [PubMed]
110. Pupeikis, J.; Willenberg, B.; Camenzind, S.L.; Benayad, A.; Camy, P.; Phillips, C.R.; Keller, U. Spatially multiplexed single-cavity dual-comb laser. *Optica* **2022**, *9*, 713–716. [CrossRef]
111. Kayes, M.I.; Abdukerim, N.; Rekik, A.; Rochette, M. Free-running mode-locked laser based dual-comb spectroscopy. *Opt. Lett.* **2018**, *43*, 5809–5812. [CrossRef]

112. Chen, J.; Zhao, X.; Yao, Z.; Li, T.; Li, Q.; Xie, S.; Liu, J.; Zheng, Z. Dual-comb spectroscopy of methane based on a free-running Erbium-doped fiber laser. *Opt. Express* **2019**, *27*, 11406–11412. [CrossRef]
113. Sterczewski, Ł.A.; Przewłoka, A.; Kaszub, W.; Sotor, J. Computational Doppler-limited dual-comb spectroscopy with a free-running all-fiber laser. *APL Photonics* **2019**, *4*, 116102. [CrossRef]
114. Chen, J.; Nitta, K.; Zhao, X.; Mizuno, T.; Minamikawa, T.; Hindle, F.; Zheng, Z.; Yasui, T. Adaptive-sampling near-Doppler-limited terahertz dual-comb spectroscopy with a free-running single-cavity fiber laser. *Adv. Photonics* **2020**, *2*, 036004. [CrossRef]
115. Tian, H.; Li, R.; Endo, T.; Kato, T.; Asahara, A.; Sterczewski, L.A.; Minoshima, K. Dual-comb spectroscopy using free-running mechanical sharing dual-comb fiber lasers. *Appl. Phys. Lett.* **2022**, *121*, 211104. [CrossRef]
116. Qin, Y.; Cromey, B.; Batjargal, O.; Kieu, K. All-fiber single-cavity dual-comb for coherent anti-Stokes Raman scattering spectroscopy based on spectral focusing. *Opt. Lett.* **2021**, *46*, 146–149. [CrossRef] [PubMed]
117. Xu, K.; Ma, L.; Chen, J.; Zhao, X.; Wang, Q.; Kan, R.; Zheng, Z.; Ren, W. Dual-comb spectroscopy for laminar premixed flames with a free-running fiber laser. *Combust. Sci. Technol.* **2022**, *194*, 2523–2538. [CrossRef]
118. Andral, U.; Fodil, R.S.; Amrani, F.; Billard, F.; Hertz, E.; Grelu, P. Fiber laser mode locked through an evolutionary algorithm. *Optica* **2015**, *2*, 275–278. [CrossRef]
119. Woodward, R.; Kelleher, E.J. Towards 'smart lasers': self-optimisation of an ultrafast pulse source using a genetic algorithm. *Sci. Rep.* **2016**, *6*, 37616. [CrossRef]
120. Liao, R.; Tian, H.; Liu, W.; Li, R.; Song, Y.; Hu, M. Dual-comb generation from a single laser source: principles and spectroscopic applications towards mid-IR—A review. *J. Phys. Photonics* **2020**, *2*, 042006. [CrossRef]
121. Xie, C.; Dinno, M.A.; Li, Y.q. Near-infrared Raman spectroscopy of single optically trapped biological cells. *Opt. Lett.* **2002**, *27*, 249–251. [CrossRef]